

Simulation and Analysis of Chatter Onset in Orthogonal Cutting Process Using an Energy-Based Approach

Mohammad Ghorbani^{1,*}, Mostafa Sarjoughian²

¹ Assist. Prof., Department of Mechanical Engineering, Shahreza Campus, University of Isfahan, Iran.

² BSc Graduate, Department of Mechanical Engineering, Shahreza Campus, University of Isfahan, Iran.

*Corresponding m.ghorbani@shr.ui.ac.ir

Received: 04/26/2025 Revised: 09/18/2025 Accepted: 10/07/2025

Abstract

This paper simulates workpiece vibrations in the orthogonal cutting process, from the initial engagement of the tool and workpiece to conduct an in-depth investigation of chatter onset using an energy-based approach. For this purpose, the orthogonal cutting process of a disk is divided into two distinct stages: the first revolution of the workpiece and the subsequent revolutions. The governing vibration equations for each stage are derived separately. The first-stage equation is solved analytically, while the second-stage equation is solved using the semi-discretization method. Additionally, formulations for calculating the power and energy transmitted by the cutting force and dissipated due to system damping are presented. Through simulations, a comprehensive analysis of the system's vibrational behavior during the initial revolutions of the workpiece is conducted. The findings indicate that the system behavior during the first three revolutions, regardless of cutting width, is determined by the transient response in the first revolution caused by the tool feed. Furthermore, the results show that in the stable condition, the total power is zero; in the critically stable condition, it oscillates with a constant amplitude and a zero average value; and in the unstable condition, it oscillates with an increasing amplitude and a zero average value.

Keywords: Simulation, Chatter, Orthogonal Cutting, Energy Approach.

1. Introduction

The occurrence of vibrations in machining processes is inevitable, as the flexibility of one or more components—such as the machine tool, cutting tool, and workpiece—combined with time-varying forces, creates mechanical conditions conducive to vibrations, even if their amplitude is small. These vibrations not only reduce dimensional accuracy, surface quality, and process efficiency but also accelerate tool wear, shorten tool life, cause damage to machine components, and increase maintenance costs [1,2]. In machining processes, three types of vibrations can occur: free, forced, and chatter. Among them, chatter is a form of self-excited vibration caused by the internal feedback mechanisms of the cutting process itself, without any external source of excitation.

Wave regeneration, friction, and mode coupling are the three primary mechanisms responsible for chatter vibration and instability in machining processes [3]. Among these, wave regeneration is considered the most significant contributor to vibration-induced instability. In this mechanism, surface undulations left on the workpiece from previous tool passes overlap with those generated in subsequent passes. This overlap amplifies the dynamic chip thickness and cutting forces,

ultimately leading to instability in the machining process [4].

Orthogonal cutting, as a simplified and two-dimensional model of the chip formation process, is suitable for investigating various phenomena in machining processes, including chatter vibration. Several studies have been conducted to explore vibrations in this process. A review of previous research shows that their main focus has been either on identifying the stability state of the process under different machining parameters or on numerically solving the equations governing system vibrations, while typically ignoring the system behavior during the first revolution of the workpiece. In other words, modeling the process from the initial engagement between the tool and the workpiece until the system reaches a stable or unstable state has not been addressed by dividing the cutting process into a turning stage on a smooth surface and a turning stage on a previously machined surface. Moreover, the variations in power and energy transmitted to the system by the cutting force, as well as the energy dissipated through system damping, have not been analyzed with the aim of describing the physical behavior of the system under different stability conditions. In this paper, the

orthogonal cutting process of a disk is modeled starting from the moment the tool begins to engage the workpiece. By deriving and solving the governing vibration equations, the time response of the system during the first and subsequent revolutions of the workpiece is calculated, and the vibration behavior during the initial revolutions is analyzed in depth. Additionally, the changes in system power and energy under different stability conditions are investigated and interpreted. The results are validated by comparison with examples available in the literature.

2. Modeling

2.1. Vibration Modeling of the Orthogonal Cutting Process

Figure 1 shows a schematic representation of the dynamics of the orthogonal cutting process. A disk with thickness a is being cut by a cutting tool that spans its entire width. The vibrational displacement of the workpiece is denoted by x , while the equivalent flexibility and damping of the system in the direction of tool feed are modeled using a spring with stiffness k_x and a damper with damping coefficient c_x , respectively.

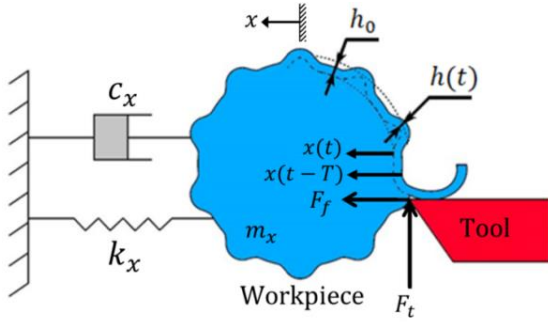


Figure 1. 1-DOF vibration model showing the forces acting on the workpiece and illustrating the wave regeneration mechanism

If there is no vibration in the system, in other words, if a chip of constant thickness h_0 is removed from the workpiece by the tool, the force acting on the workpiece in the direction of tool feed can be expressed using the mechanistic model as follows [5]:

$$F_f = K_f a h_0 \quad (1)$$

where K_f in (1) is the cutting coefficient of the workpiece material in the feed direction. Due to the system flexibility, when the tool and workpiece begin to engage, vibrations of the workpiece in the feed direction lead to variations in the chip thickness. During the first revolution, when the tool is removing material from a smooth surface, the dynamic chip thickness is calculated as follows:

$$h(t) = f(t) - x(t) \quad (2)$$

where $f(t)$ represents the tool feed, and $x(t)$ denotes the workpiece vibration in the feed direction. It is important

to note that during the first revolution of the workpiece, the tool feed increases from zero at the moment of engagement to h_0 by the end of the revolution. Under these conditions, the feed force and the governing equation for workpiece vibration can be expressed as follows:

$$F_f(t) = K_f a h(t) = K_f a (f(t) - x(t)) \quad (3)$$

$$m_x \ddot{x} + c_x \dot{x} + k_x x = K_f a (f(t) - x(t)) \quad (4)$$

$$f(t) = \frac{h_0}{T} t, \quad (0 \leq t \leq T) \quad (5)$$

where m_x , c_x , and k_x represent the mass, equivalent damping, and equivalent stiffness of the workpiece in the feed direction, respectively. In (5), T denotes the spindle revolution period, which is calculated by $T = 60 / \Omega_s$, where Ω_s is the spindle revolution speed in revolutions per minute (RPM).

In the second and subsequent revolutions of the workpiece, chip removal occurs from a wavy surface. As a result, the dynamic chip thickness and the governing equation for workpiece vibrations are expressed as follows [5]:

$$h(t) = h_0 - [x(t) - x(t - T)] \quad (6)$$

$$m_x \ddot{x} + c_x \dot{x} + k_x x = K_f a h_0 - K_f a [x(t) - x(t - T)] \quad (7)$$

where $x(t - T)$ represents the vibration of the workpiece in the previous workpiece revolution. It is evident that, in order to determine the time response of the system during the second and subsequent revolutions, the time response of the system during the first revolution of the workpiece must be known.

2.2. Solving the Governing Equation of Workpiece Vibrations During the First Revolution

By combining (4) and (5), the equation governing the vibrations of the workpiece during the first revolution is rewritten as follows:

$$m_x \ddot{x} + c_x \dot{x} + (k_x + K_f a)x = \frac{K_f a h_0}{T} t, \quad (0 \leq t \leq T) \quad (8)$$

The general solution of the differential equation (8) consists of a homogeneous (transient) part and a particular part. By applying zero initial conditions, i.e., $x(0) = \dot{x}(0) = 0$, the solution is obtained as follows:

$$\begin{aligned} x(t) &= x_h(t) + x_p(t) \\ x_h(t) &= e^{-\xi \Omega_n t} [A \cos(\Omega_d t) + B \sin(\Omega_d t)], \\ x_p(t) &= Ct + D, \\ \Omega_n &= \sqrt{\frac{k_x + K_f a}{m_x}}, \quad \xi = \frac{c_x}{2m_x \Omega_n}, \end{aligned} \quad (9)$$

$$\Omega_d = \Omega_n \sqrt{1 - \xi^2}, \quad C = \frac{K_f a h_0}{T(k_x + K_f a)},$$

$$D = -\frac{c_x K_f a h_0}{T(k_x + K_f a)^2}, \quad A = -D,$$

$$B = -\frac{C + \xi \Omega_n D}{\Omega_d}$$

where Ω_n is the natural frequency of the system, ξ is the damping ratio, and Ω_d is the damped natural frequency.

2.3. Solving the Governing Equation of Workpiece Vibrations in Subsequent Revolutions

In the second and subsequent revolutions of the workpiece (i.e., $t > T$), the system vibrations are governed by the delayed differential equation (7). To solve this equation and obtain the time response, the semi-discretization method is employed here. By defining the undamped natural frequency of the machine tool as $\omega_n = \sqrt{k_x/m_x}$ and the damping ratio as $\zeta = c_x/(2m_x\omega_n)$, (7) is rewritten as follows [6]:

$$\ddot{x} + 2\zeta\omega_n\dot{x} + \omega_n^2x = \frac{\omega_n^2}{k_x}K_fah_0 - \frac{\omega_n^2}{k_x}K_fa[x(t) - x(t-T)], \quad (t > T) \quad (10)$$

Equation (10) can be expressed in state space form as follows [6]:

$$\begin{aligned} x_1(t) &= x(t), \quad x_2(t) = \dot{x}(t), \quad \dot{x}_1(t) = x_2(t) \\ \dot{x}_2(t) &= \frac{\omega_n^2}{k_x}K_fah_0 - \frac{\omega_n^2}{k_x}K_fa[x_1(t) - x_1(t-T)] - 2\zeta\omega_nx_2(t) \end{aligned} \quad (11)$$

By expressing (11) in matrix form, the following relationship is obtained [6]:

$$\begin{aligned} \dot{y}(t) &= Ly(t) + Ry(t-T) + f_0, \\ y(t) &= \begin{Bmatrix} x_1(t) \\ x_2(t) \end{Bmatrix}, \quad y(t-T) = \begin{Bmatrix} x_1(t-T) \\ x_2(t-T) \end{Bmatrix} \\ L &= \begin{bmatrix} 0 & 1 \\ -\frac{\omega_n^2}{k_x}(K_fa + k_x) & -2\zeta\omega_n \end{bmatrix} \\ R &= \begin{bmatrix} 0 & 0 \\ \frac{\omega_n^2}{k_x}K_fa & 0 \end{bmatrix}, \quad f_0 = \begin{Bmatrix} 0 \\ \frac{\omega_n^2}{k_x}K_fah_0 \end{Bmatrix} \end{aligned} \quad (12)$$

To solve the differential equation (12) using the semi-discretization method, the period T is divided into m subdivisions, such that $T = m\Delta t$. Then the response of the system in the i -th subdivision is calculated as follows [6]:

$$\begin{aligned} y_{i+1} &= e^{L\Delta t}y_i + \frac{1}{2}(e^{L\Delta t} - I)L^{-1}R(y_{i-m} \\ &\quad + y_{i-m+1}) + (e^{L\Delta t} - I)L^{-1}f_0, \quad (i > m) \end{aligned} \quad (13)$$

where I denotes the identity matrix.

2.4. Calculation of the Vibrational Power and Energy of the System

Given the time response $x(t)$ of the system under regenerative vibrations, the dynamic chip thickness $h(t)$ and the force $F_x(t)$ applied to the workpiece can be calculated as follows:

$$h(t) = \begin{cases} \frac{h_0}{T}t - x(t), & 0 \leq t \leq T \\ h_0 - [x(t) - x(t-T)], & t > T \end{cases} \quad (14)$$

$$F_x(t) = K_fah(t) \quad (15)$$

According to the definition of power, which is the dot product of force and velocity at the point of application, the power transmitted to the workpiece by the cutting force and the power dissipated by the system's damping can be calculated using the following equations:

$$P_f(t) = F_x(t)\dot{x}(t) \quad (16)$$

$$P_c(t) = -[c_x\dot{x}(t)]\dot{x}(t) \quad (17)$$

The negative sign in (17) is included to account for the fact that the damper force always acts in the opposite direction of the velocity. In fact, the negative sign represents the energy loss due to damping. The sum of the two powers, $P_f(t)$ and $P_c(t)$, represents the total power input to the system at any given instant:

$$P(t) = P_f(t) + P_c(t) \quad (18)$$

If the total power $P(t)$ is positive, it indicates energy injection into the system, while if it is negative, it indicates energy dissipation from the system. The total energy input to the system from time zero to time t can be obtained by integrating the power $P(t)$:

$$E(t) = \int_0^t P(\tau)d\tau \quad (19)$$

Given that the values of $x(t)$ and $\dot{x}(t)$ were calculated in a discrete manner in the previous section, numerical integration can be used to calculate the integral in (19). By examining the changes in the power calculated from (18) or the energy from (19), the stability state of the system can be determined. If the energy input to the system remains within a limited value over time, the system will remain in a stable state. However, if the energy input increases over time, the amplitude of the system's vibrations will also increase, leading to instability.

3. Results and Discussion

In the dynamic model of the process, the damper force always acts in the opposite direction to the mass motion, and its work is always negative, indicating energy loss from the system. Although the cutting force $F_x(t)$ also acts in the positive direction, its work can be either positive or negative depending on the direction

of mass motion, and thus, it can serve as a factor for either injecting or extracting energy from the system. Therefore, in this section, the terms energy injection, energy extraction, and energy dissipation are used to refer to the positive work of the cutting force, the negative work of the cutting force, and the dissipated energy of the damper, respectively. Since the amplitude of mass vibrations at any given moment is influenced by the amount of system energy, the sum of the injected, extracted, and dissipated energies over time determines the stability of the system. Furthermore, given that there are no other energy injection or absorption factors in the system, the total energy from the moment the motion begins until any desired moment is equal to the energy of the entire system, that is, the sum of the kinetic and potential energies up to that point. In this section, using the vibration and shear parameters presented in Table 1, the results related to the system's power and energy are presented and discussed.

Table 1. Vibration and shear parameters used in numerical simulations [7]

m_x (kg)	c_x (N.s/m)	k_x (N/m)	K_f (N/m ²)
0.561	145	6.48×10^6	1384×10^6

Figure 2 shows the changes in the power and energy of the system over time in the steady state condition. In this figure, the solid line represents the instantaneous changes, while the dashed line represents the average power and energy. It can be seen that during the first revolution of the workpiece, the instantaneous power fluctuates positively, and as a result, the system's energy, which is represented by the area under the power-time curve, increases during this round. Although the dissipated power of the damper is always negative, Figure 2(a) shows that in the first revolution, the power injected by the cutting force is consistently greater than the dissipated power of the damper. This injected power, which causes the upward increase in the systems energy, is actually stored as potential energy in the spring and causes it to deform until the system nears its equilibrium point.

In the second revolution of the workpiece, the instantaneous power oscillates with both positive and negative amplitudes but maintains a positive average value. As a result, the system's energy increases slightly and oscillates. In this cycle, the energy injected into the system by the cutting force exceeds the sum of the energy extracted by the cutting force and the energy dissipated by the damper.

In the third revolution, the instantaneous power oscillates around zero, with its amplitude remaining nearly constant. This indicates that, during this cycle, the total energy injected, extracted, and dissipated is balanced, and the system's energy remains at the same level, exhibiting oscillatory behavior with nearly constant amplitude. From the fourth revolution onward, the instantaneous power oscillates with an average value of zero, and its amplitude decreases

exponentially. Similarly, the system's energy oscillates around its previous average value, with its amplitude diminishing over time until it stabilizes at a constant level. In fact, from the fourth revolution onward, the total energy dissipated and extracted exceeds the energy injected into the system. As energy is dissipated by the damper, the amplitude of the mass vibrations decreases, and the system eventually stabilizes at its equilibrium point.

In Figure 3, the changes in power and energy are shown for the critically stable condition. While the behavior of the graphs during the first to third revolutions is similar to that of the stable condition, from the beginning of the fourth revolution onward, the instantaneous power oscillates with a constant amplitude around zero. As a result, the system's energy also oscillates around its average value with a constant amplitude. In this case, the sum of the energy injected into the system, extracted from it, and dissipated during one oscillation cycle is zero. This equal exchange of energy causes the system to oscillate with a constant amplitude around its equilibrium point.

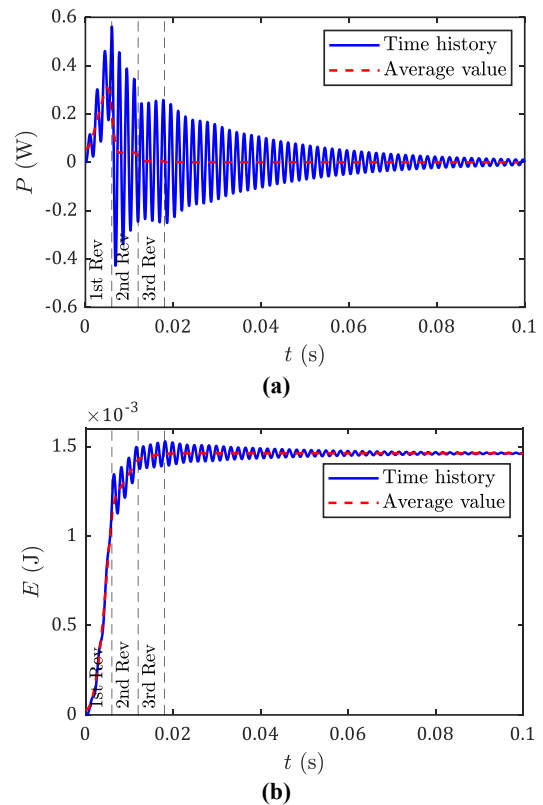
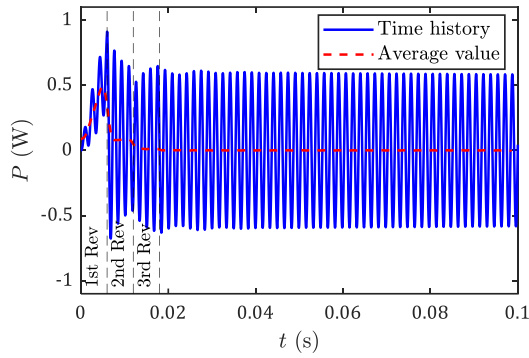
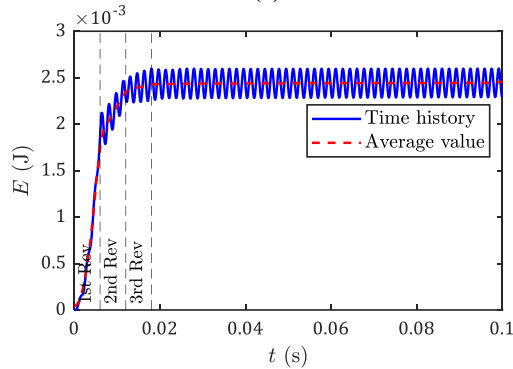


Figure 2. (a) Power changes over time with its average value, (b) Energy changes over time with its average value (stable with $\Omega_s = 10,000$ rpm, $h_0 = 0.2$ mm, $a = 0.5$ mm)



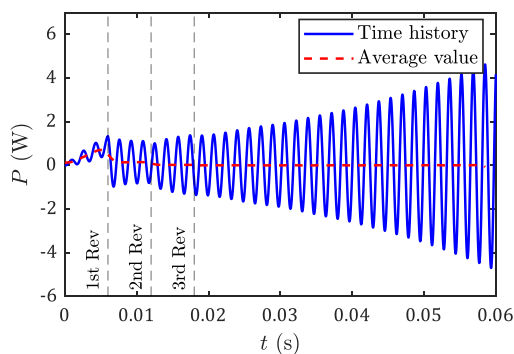
(a)



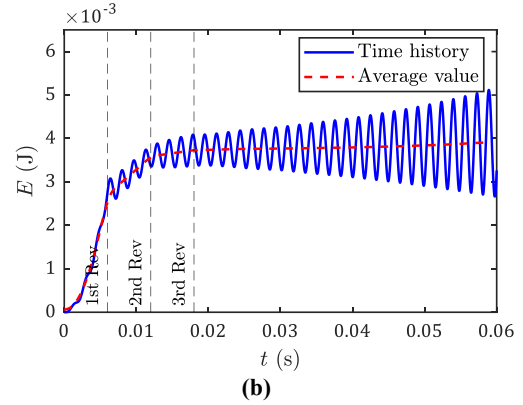
(b)

Figure 3. (a) Power changes over time with its average value, (b) Energy changes over time with its average value (critically stable with $\Omega_s = 10,000 \text{ rpm}$, $h_0 = 0.2 \text{ mm}$, $a = 0.645 \text{ mm}$)

In Figure 4, the changes in the power and energy of the system are shown for the unstable condition. As with the stable condition, the changes in the graphs during the first three revolutions are similar. However, from the fourth revolution onward, the instantaneous power oscillates with an increasing amplitude around zero, and the system's energy also oscillates around its average value with an increasing amplitude. In this case, the energy injected into the system exceeds the total energy extracted and dissipated during each cycle. This continuous increase in the system's energy causes the amplitude of vibrations to grow progressively, indicating an unstable condition.



(a)



(b)

Figure 4. (a) Power changes over time with its average value, (b) Energy changes over time with its average value (unstable with $\Omega_s = 10,000 \text{ rpm}$, $h_0 = 0.2 \text{ mm}$, $a = 0.8 \text{ mm}$)

4. Conclusions

In this paper, the chatter phenomenon in the orthogonal cutting process was investigated and simulated using an energy-based approach. By employing a vibration model, the system dynamics were analyzed in detail across two stages: the first revolution of the workpiece and the subsequent revolution cycles. Using the time-domain responses, the power and energy of the system, generated by the cutting force and dissipated by the damper, were calculated. An in-depth analysis of the vibration responses revealed that the system's behavior during the first three revolutions of the workpiece depends significantly on the interaction between the tool feed and the vibrations of the workpiece and is relatively unaffected by the cutting parameters. In subsequent revolution cycles, the changes in power and energy are influenced by the cutting parameters.

In the stable condition, the instantaneous power oscillates with decreasing amplitude around zero, and the system energy converges to a constant value. At the critically stable condition, the instantaneous power oscillates with a constant amplitude around zero, with the system energy also displaying oscillatory behavior with a constant amplitude. In the unstable condition, the instantaneous power oscillates with increasing amplitude around zero, and the system energy exhibits oscillatory behavior with an increasing amplitude. These findings not only provide a deeper understanding of the dynamic behavior of the system and the vibration mechanism in the turning process but also demonstrate that accurate modeling and analysis of system behavior in the time domain, using an energy-based approach, can serve as an effective tool for simulating and predicting process stability under various conditions.

5. References

- [1] Yuan L, Pan Z, Ding D, Sun S, Li W (2018) A review on chatter in robotic machining process regarding both regenerative and mode coupling mechanism. *IEEE/ASME Trans Mechatronics* 23(5): 2240-2251.

- [2] Pour M, Aliabadi A, Rahman nia S (2015) Identifying Process Damping of Turning Process Using Time Series Analysis. *J Solid Fluid Mech* 5(4): 35-45.
- [3] Wiercigroch M, Budak E (2001) Sources of nonlinearities, chatter generation and suppression in metal cutting. *Philos Trans R Soc Lond A* 359(1781): 663-693.
- [4] Dong X, Shen X, Fu Z (2021) Stability analysis in turning with variable spindle speed based on the reconstructed semi-discretization method. *Int J Adv Manuf Technol* 117(11-12): 3393-3403.
- [5] Altintas Y, Weck M (2004) Chatter stability of metal cutting and grinding. *CIRP Ann-Manuf Technol* 53(2): 619-242.
- [6] Insperger T, Stepan, G (2002) Semi-discretization method for delayed systems. *Int J Numer Methods Eng* 55(5): 503-518.
- [7] Altintas Y, Eynian M, Onozuka H (2008) Identification of dynamic cutting force coefficients and chatter stability with process damping. *CIRP Ann-Manuf Technol* 57(1): 371-374.